Theoretical Study on the Reaction Mechanism of the Gas-Phase $H_2/CO_2/Ni(^3D)$ System

Song Qin, Changwei Hu,* Huaqing Yang, and Zhishan Su

Key Laboratory of Green Chemistry and Technology (Sichuan University), Ministry of Education, College of Chemistry, Sichuan University, Chengdu, Sichuan, 610064, China

Received: February 7, 2005; In Final Form: May 27, 2005

The ground-state potential energy surface (PES) in the gas-phase $H_2/CO_2/Ni(^3D)$ system is investigated at the CCSD(T)//B3LYP/6-311+G(2d,2p) levels in order to explore the possible reaction mechanism of the reverse water gas shift reaction catalyzed by $Ni(^3D)$. The calculations predict that the C−O bond cleavage of CO_2 assisted by co-interacted H_2 is prior to the dissociation of the H_2, and the most feasible reaction path for $Ni(^3D) + H_2 + CO_2 \rightarrow Ni(^3D) + H_2O + CO$ is endothermic by 12.5 kJ mol^{-1} with an energy barrier of 103.9 kJ mol^{-1}. The rate-determining step for the overall reaction is predicted to be the hydrogen migration with water formation. The promotion effect of H_2 on the cleavage of C−O bond in CO_2 is also discussed and compared with the analoguous reaction of $Ni(^3D) + CO_2 \rightarrow NiO + CO$, and the difference between triplet and singlet $H_2/CO_2/Ni$ systems is also discussed.

1. Introduction

The hydrogenation of CO_2 usually reaches the production of CH_4 on transition metal catalysts under fairly mild reaction conditions,[1−3] but its mechanism is still in dispute.[4−6] Some previous experimental studies[7−11] supported the mechanism involving the conversion of CO_2 to CO via the reverse water gas shift (RWGS) reaction followed by CO hydrogenation. On the other hand, the water gas shift (WGS) reaction and its reverse reaction are also of considerable industrial importance.[12] Since Ni-based catalysts play a particularly effective role in both catalytic processes, and it is widely considered that the coordination of CO_2 to metal centers would be the key step for the activation of CO_2, the system of $Ni + CO_2$ has therefore become one of the hotly investigated theoretical and experimental topics.[13−23]

Theoretical investigation aimed at a reaction mechanism in the gas phase has shown to be a useful tool. Although the real reaction usually occurs on heterogeneous catalysts, the investigation on the gas-phase reaction of small molecules as model catalysts has been considered capable of providing a wealth of inner insight into the nature of real catalytic reactions.[23−29] To our knowledge, there is no literature based on a quantum chemistry approach aimed at the mechanism of the RWGS reaction over Ni catalyst. The theoretical efforts most closely related to this area are still restricted to metal + CO_2 systems.[19−23,30−33] Hannachi et al.[22] proposed that the entire triplet-state $Ni + CO_2 \rightarrow NiO + CO$ reaction involves Ni insertion into the C−O bond of CO_2, and that the oxygen abstraction and Ni insertion take place simultaneously with electron transfer from Ni to CO_2. Similar reaction mechanisms in $Ti + CO_2$[34] and $Sc + CO_2$[35,36] systems also revealed that the metal insertion process may be accompanied by the $3d-\pi^*$ orbital interaction between the transition metal and carbon dioxide. Our recent theoretical investigation on the gas-phase $H_2/CO_2/Ni(^1S)$ system suggested that the addition of H_2 facilitated the insertion of Ni into the C−O bond of CO_2 via $\sigma \rightarrow \pi^*$ interaction.[23]

* Corresponding author. E-mail: gchem@scu.edu.cn, chwehu@mail.sc.cninfo.net.

In the present paper, the ground-state gas-phase $H_2/CO_2/Ni(^3D)$ system is studied using CCSD(T)//B3LYP methods to find the possible reaction mechanism of the RWGS reaction over the $Ni(^3D)$ catalyst, and the promotion effect of H_2 on the entire reaction mechanism is also discussed. The above work is expected to obtain an essential piece of information for a better understanding of the reaction mechanism as well as for the design of new catalysts.

2. Computational Details

The geometries of all stationary points (reactants, products, intermediates, and transition states) on the triplet-state potential energy surface (PES) for the $H_2/CO_2/Ni(^3D)$ system are optimized at the B3LYP/6-311+G(2d,2p) level.[37−39] Vibrational frequencies are calculated at the B3LYP/6-311+G(2d,2p) level to check whether the obtained stationary point is an intermediate or first-order transition state and scaled by 0.963 to correct the overestimation as well as to obtain the zero-point-energy (ZPE) correlation.[40] For each transition state, intrinsic reaction coordinate (IRC)[41] calculations were performed in both directions to connect these corresponding intermediates at the above level. A step of 0.1 amu$^{1/2}$ bohr is used in the IRC procedure. The stability of the wave function was checked for each stationary point in the RWGS reaction.

In addition, the single-point energies are also performed at the CCSD(T)/6-311+G(2d,2p) level at the B3LYP optimized geometries. This correlation treatment in the coupled cluster calculations involves all valence electrons and is expected to obtain more reliable relative energies.[42,43] Unless otherwise specified, the CCSD(T) single-point energies are used in the following discussions.

All calculations in the present study were performed using the Gaussian 03 program.[44]

3. Results and Discussion

The optimized structures of various species on the triplet-state potential energy curve of the reaction of $Ni(^3D) + H_2 + CO_2$ are depicted in Figure 1. The relative energies of various

10.1021/jp0506585 CCC: $30.25
Published on Web 07/01/2005

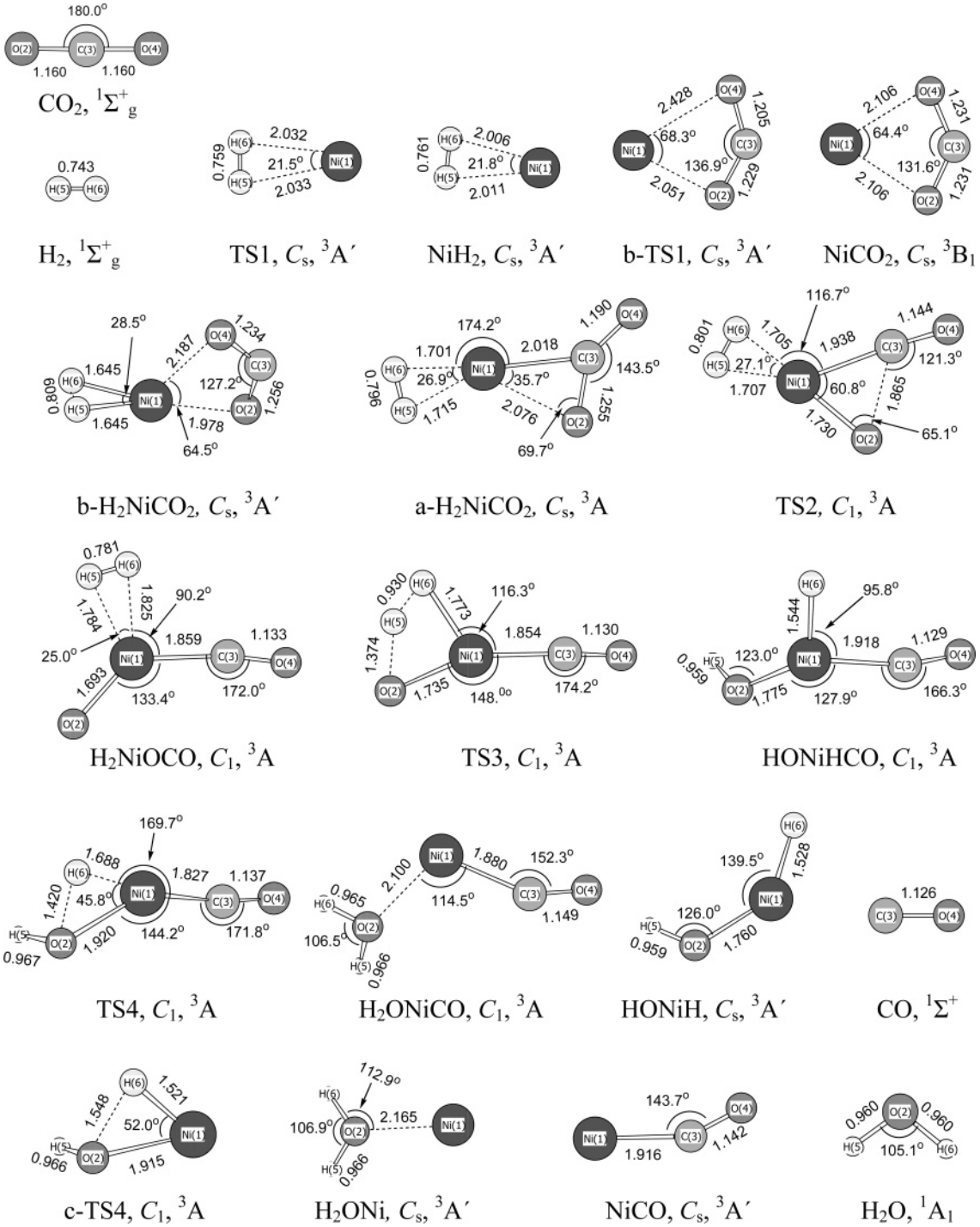

Figure 1. Geometries of various species on PES of RWGS reaction in the $H_2/CO_2/Ni(^3D)$ system, optimized at B3LYP/6-311+G(2d,2p) level. Bond lengths are in angstroms, and angles are in degrees.

species in the above reaction calculated at the CCSD(T)//B3LYP/6-311+G(2d,2p) levels are listed in Table 1. The energy diagram along the triplet reaction pathway of various species obtained from CCSD(T)/6-311+G(2d,2p) single-point calculations is shown in Figure 2.

3.1. Formation of H_2NiCO_2 Co-complex. It is shown that there exist two distinct co-complexes H_2NiCO_2 along the predicted reaction paths, which are marked as a-H_2NiCO_2 and b-H_2NiCO_2, respectively. It is predicted that the formation of the two co-complexes is closely dependent on the coordination sequence of CO_2 and H_2 to Ni. That is, if H_2 interacts first with Ni, and the resulting system interacts with CO_2, a-H_2NiCO_2 and b-H_2NiCO_2 may form; whereas, if CO_2 interacts first with Ni, and the resulting stable system interacts with H_2, only b-H_2NiCO_2 will be obtained. Although the co-complex b-H_2NiCO_2 is identified as a stable species, we have failed to locate any transition state connecting it with a-H_2NiCO_2 or other intermediates on the reaction path for C−O bond cleavage. Therefore, according to the data obtained in the present work, the entire $Ni(^3D) + H_2 + CO_2 \rightarrow Ni(^3D) + H_2O + CO$ reaction proceeds via the formation of the co-complex a-H_2NiCO_2 instead of b-H_2NiCO_2.

As shown in Figure 1, in the co-complex a-H_2NiCO_2, two bonds between Ni and the C and O(2) atoms of the CO_2 moiety form, and the OCO angle has been distorted to 143.5° compared to the angle in free CO_2 molecule. The planar $NiCO_2$ moiety in

TABLE 1: Relative Energies (kJ mol^{-1}) in the H_2/CO_2/Ni(^{3}D) System Calculated at CCSD(T)//B3LYP/6-311+G(2d,2p) Levels

species	B3LYP	CCSD(T)
Ni(^{3}D) + H_2 + CO_2	0.0	0.0
TS1 + CO_2	6.9	11.5
NiH_2 + CO_2	8.9	10.1
a-H_2NiCO_2	14.4	2.6
b-TS1	69.4	77.3
$NiCO_2$	68.4	63.7
b-H_2NiCO_2	17.9	−8.4
TS2	119.5	85.9
H_2NiOCO	53.2	21.7
TS3	98.5	75.4
HONiHCO	−55.2	−87.1
TS4	39.1	16.8
H_2ONiCO	−34.7	−81.3
HONiH + CO	−9.5	−50.4
c-TS4 + CO	145.4	119.1
H_2ONi + CO	39.8	−13.1
NiCO + H_2O	−4.2	−28.6
Ni(^{3}D) + CO + H_2O	56.0	12.5

this co-complex is almost the same as that in the $\eta^2_{C,O}$-$NiCO_2$ complex. Galan et al.[20] and Hannachi et al.[22] suggested that this triplet $\eta^2_{C,O}$-$NiCO_2$ complex should be a unstable species in the triplet-state gas-phase CO_2/Ni system. The location of the triplet-state $\eta^2_{C,O}$-$NiCO_2$ as a stationary structure was also failed in the present work. Our calculations show that the addition of H_2 molecule can stabilize the triplet-state $\eta^2_{C,O}$-$NiCO_2$ by the formation of the a-H_2NiCO_2 co-complex. CCSD(T) calculations indicated that the addition of CO_2 to the NiH_2 species give a stabilization energy of 7.5 kJ mol^{-1} relative to the NiH_2 + CO_2 species.

For the co-complex b-H_2NiCO_2, two O-ends of the CO_2 moiety attach to Ni with the formation of the cyclic four-membered $NiCO_2$ ring, which is in general similar to the triplet-state $\eta^2_{O,O}$-$NiCO_2$ complex. Previous theoretical research[20−22] identified this $\eta^2_{O,O}$-$NiCO_2$ complex as a stable complex in the triplet-state gas-phase CO_2/Ni system. The calculations in the present work further indicate that the presence of H_2 stabilizes this co-complex by 72.1 kJ mol^{-1}.

3.2. H_2-Promoted C−O Bond Cleavage of CO_2 by Ni Insertion. From a-H_2NiCO_2, the reaction proceeds by Ni insertion into one C−O bond of the CO_2 moiety via transition state TS2. For TS2, as shown in Figure 1, the C−O(2) distance is remarkably longer than that for a-H_2NiCO_2. The Ni−O(2) distance becomes shorter than that for a-H_2NiCO_2. These results indicate that the interaction of Ni−O(2) has been enhanced and the C−O(2) bond has been significantly activated. Thus, this reaction step involves the cleavage of the C−O(2) bond and leads to the formation of CO fragment forming H_2NiOCO. In H_2NiOCO, as shown in Figure 1, the C−O(2) bond has been cleaved. As to the H_2 moiety, its structure has not been significantly changed, indicating that the H_2 moiety remains undissociated on interacting with Ni. CCSD(T) calculations give an endothermicity of about 19.1 kJ mol^{-1} and an energy barrier of 83.3 kJ mol^{-1} for this step.

Hannachi et al.[22] proposed that the most feasible reaction of Ni(^{3}D) + CO_2 → NiO + CO involves the Ni insertion process with energy barriers of 144.6 and 188.1 kJ mol^{-1} for ^{3}A″ and ^{3}A′ PESs, respectively. In our present H_2/CO_2/Ni(^{3}D) system, only one triplet-state PES is obtained as a result of the degeneration of orbital symmetry originating from the presence of H_2. We visualize the SOMOs (singly occupied molecular orbitals) of H_2NiOCO in Figure 3. As shown in Figure 3, these orbitals can be characterized as mostly π* NiO orbitals. This characterizes the electronic configuration of NiO moiety in H_2-NiOCO to be the $^3\Sigma$ ($1\sigma^2 1\pi^4 2\delta^4 2\sigma^2 2\pi^2$) state. Since the reaction path yielding the $^3\Sigma$ state NiO moiety corresponds to the ^{3}A″ surface in the CO_2/Ni(^{3}D) system in Hannachi's research, the present triplet RWGS reaction PES is therefore more compatible with the ^{3}A″ PES in the CO_2/Ni(^{3}D) system.

Comparing the above data with the CO_2/Ni(^{3}D) system, it is found that the most obvious difference is the barrier height for the Ni insertion process. CCSD(T) calculations give the energy barrier for Ni insertion in the H_2/CO_2/Ni(^{3}D) system to be 83.3 kJ mol^{-1}, which is significantly lower than that for the analogous step on the ^{3}A″ surface in the CO_2/Ni(^{3}D) system (144.6 kJ mol^{-1}). For comparison, we have also reproduced the corresponding transition state TS(^{3}A″) in the CO_2/Ni(^{3}D) system reported in ref 22 at the B3LYP/6-311+G(2d) level, and visualized the orbital interaction in the above transition states. The visualizations of orbital interactions in TS(^{3}A″) and TS2(^{3}A) are plotted in Figure 4.

Hannachi et al.[22] also suggested that the process of Ni insertion with cleavage of the C−O bond involves charge

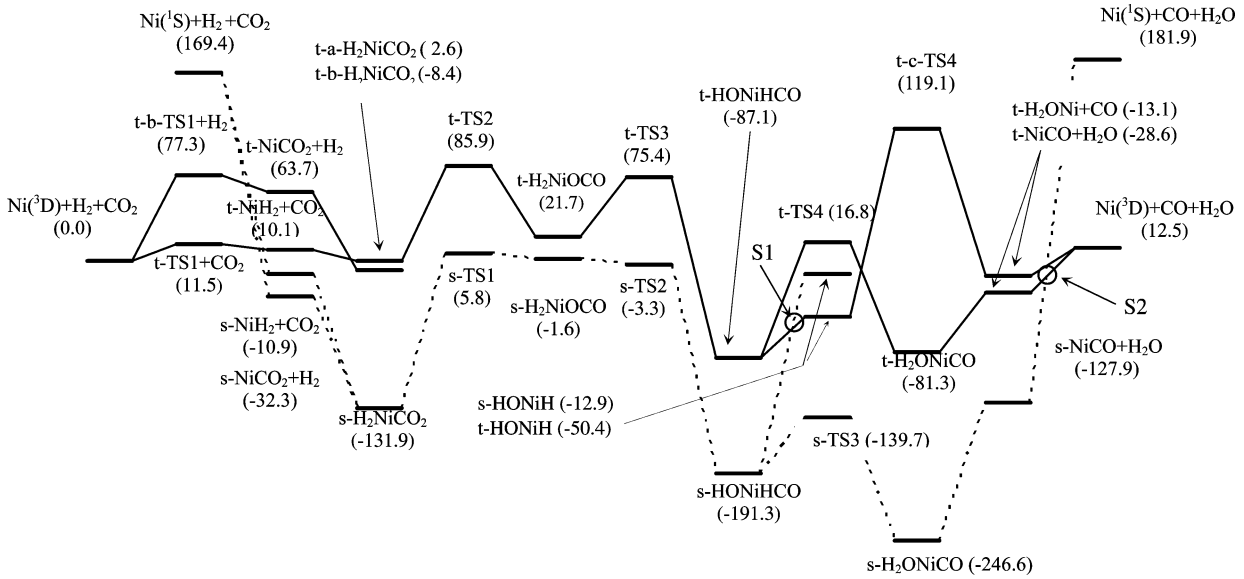

Figure 2. Potential energy profile for RWGS reaction in triplet (t) and singlet (s)[23] state H_2/CO_2/Ni systems calculated at CCSD(T)//B3LYP/6-311+G(2d,2p) levels. The CCSD(T) single-point relative energies (kJ mol^{-1}) are listed in parentheses.

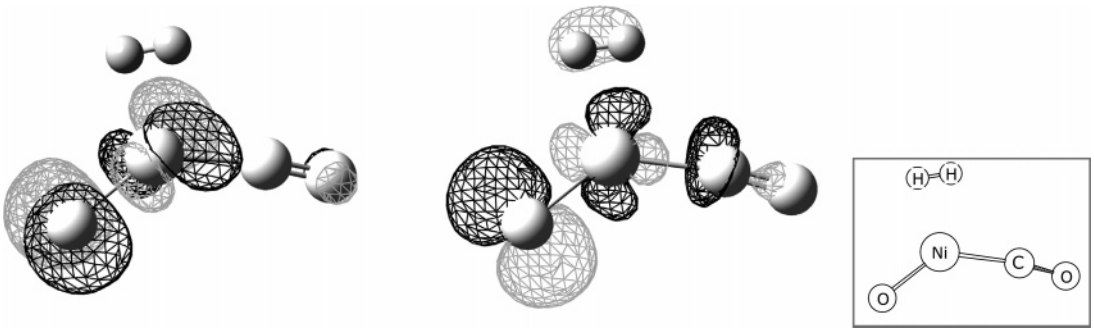

Figure 3. Visualization of SOMOs in H_2NiOCO.

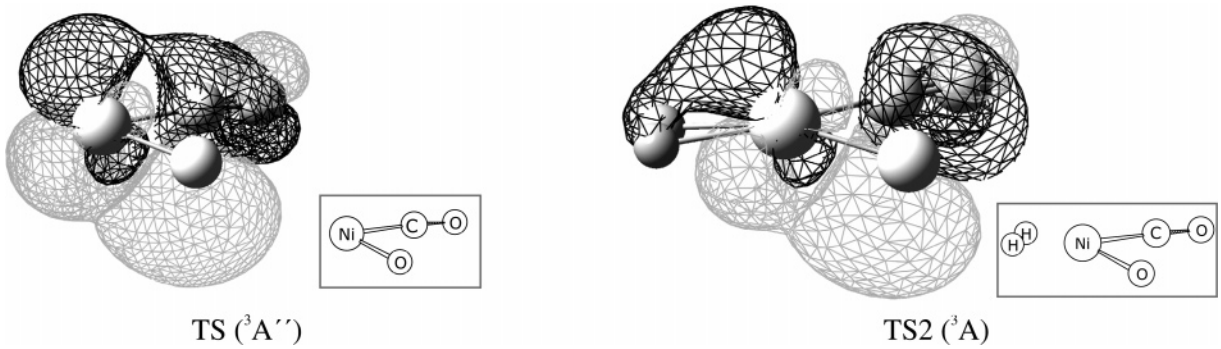

Figure 4. Visualization of orbital interaction of comparable transition states in $CO_2/Ni(^3D)$ and $H_2/CO_2/Ni(^3D)$ systems, respectively.

transfer from Ni to the π^* orbital of CO_2. For TS(^{3}A′′), as shown in the left of Figure 4, the 3d orbital of Ni interacts with the π^* molecular orbital (MO) of CO_2, and the charge transfer from Ni to the π^* MO of CO_2 may take place by means of this 3d−π^* orbital interaction. In the case of TS2(^{3}A), this 3d−π^* orbital interaction also exists in the $NiCO_2$ moiety, and the σ orbital of the H_2 part simultaneously interacts with the 3d orbital of Ni. Consequently, there may exist a hyperconjunctive interaction between the H_2 moiety and the Ni center (natural bond orbital analysis performed gives a large stabilization energy of 106.6 kJ mol^{-1} for BD(σ)H5−H6 → LP*(4)Ni, confirming this point of view). Hence, with such a hyperconjunctive orbital interaction, the H_2 moiety may also reinforce the 3d−π^* orbital interaction and be advantageous to the charge transfer from Ni to the π^* MO of CO_2. The enhanced charge-transfer process therefore facilitates the cleavage of C−O and makes the energy barrier height lower for this reaction step, as compared to the analogous step in the $CO_2/Ni(^3D)$ system.

3.3. Formation of H_2O + CO. After Ni insertion, the reaction proceeds via transition state TS3 to produce HONiHCO. For TS3, as shown in Figure 1, the H(5)−H(6) distance becomes longer than that for H_2NiOCO, indicating that the H(5)−H(6) bond becomes weakened. As a result, this reaction step involves the cleavage of the H(5)−H(6) bond of this H_2 moiety, which leads to the migration of H(6) from the H_2 moiety to the O(2) atom. For HONiHCO, the H(5)−H(6) distance is obviously longer than that for TS3. The above results indicate that the H_2 fragment has been remarkably activated in this structure. CCSD-(T) calculations give an exothermicity of about 108.8 kJ mol^{-1} and an energy barrier of 53.7 kJ mol^{-1} for this step.

From HONiHCO, the reaction proceeds via transition state TS4 to produce the final intermediate H_2ONiCO. For TS4, the Ni−H(5) bond becomes longer, indicating that the Ni−H(5) bond is remarkably activated in TS4. Therefore, this reaction step involves the migration of the H(5) atom from Ni and leads to the formation of water. CCSD(T) calculations give an endothermicity of 5.8 kJ mol^{-1} and an energy barrier of 103.9 kJ mol^{-1} for this step. The intermediate H_2ONiCO can release a water molecule and leave NiCO behind at an energy cost of 52.7 kJ mol^{-1} without any energy barrier. Our calculations also indicate that the NiCO can further decompose to Ni(^{3}D) + CO products at an energy cost of 41.1 kJ mol^{-1} without any energy barrier.

As shown in Figure 2, from HONiHCO, the reaction can proceed via an alternative reaction path by the decomposition of HONiHCO, forming CO and HONiH. The calculations predict that this step requires 36.7 kJ mol^{-1} without any energy barrier. Then, the reaction can proceed by the migration of H atom from the Ni center to the O atom via transition state c-TS4. This reaction step leads to the formation of H_2ONi. CCSD(T) calculations give an endothermicity of 37.3 kJ mol^{-1} and a rather large energy barrier of 169.5 kJ mol^{-1} for this step. Next, H_2ONi can further release a water molecule and leave the triple-state Ni(^{3}D) atom behind at an energy cost of 25.6 kJ mol^{-1} without any energy barrier. The largest energy barrier for this reaction path is predicted to be 169.5 kJ mol^{-1}, which is significantly larger than that for the competitive reaction path mentioned above. Thus this reaction path is harder to occur, when the competitive reaction path is considered.

The overall endothermicity of the Ni(^{3}D) + H_2 + CO_2 → Ni(^{3}D) + CO + H_2O reaction is predicted to be about 12.5 kJ mol^{-1} at the CCSD(T)/6-311+G(2d,2p) level. Because the calculated energy between HONiHCO and TS4 is 103.9 kJ mol^{-1}, which is the largest energy barrier along the most feasible reaction coordinate predicted in the present system, this step can be considered the rate-determining step (RDS) for the entire reaction, which corresponds to hydrogen migration with the formation of water.

3.4. Comparison with Singlet PES. Quantum chemistry CCSD(T)//B3LYP/6-311+G(2d,2p) calculations have been performed recently for the singlet-state PES for the RWGS reaction in the gas-phase $H_2/CO_2/Ni(^1S)$ system.[23] Compared with the energy of singlet-state Ni(^{1}S) from ref 23, CCSD(T) calculations predict the energy gap for the Ni atom (between the ^{3}D and ^{1}S

states) to be 169.4 kJ mol^{-1}, close to the experimental value of 167.0 kJ mol^{-1},[45] indicating the reasonableness of the theoretical level chosen. The entire pathway for the $CO_2 + H_2 + Ni(^1S)$ reaction can be summarized by the following stages: (1) the formation of the H_2NiCO_2 complex; (2) the insertion of Ni into the C−O bond; (3) the cleavage of H−H bond and the formation of water. Although the above singlet-state PES is to some extent similar to the present triplet-state PES, it is obvious that the reaction mechanisms are rather different from each other. First, the reaction paths leading to the formation of H_2NiCO_2 co-complex are distinguished. There exists only one H_2NiCO_2 co-complex in the singlet-state PES, and the reaction pathway leads to its formation from reactants without any transition state. Second, the RDS for the two reaction systems are also different. The Ni insertion was predicted to be the RDS for the $H_2/CO_2/Ni(^1S)$ system,[23] while the hydrogen migration is the RDS for the $H_2/CO_2/Ni(^3D)$ system.

As shown in Figure 2, the singlet and triplet PESs may encounter two spin crossings (S1 and S2) near the exit channel of the RWGS reactions, which correspond to the formation of products of HONiH + CO and Ni + CO + H_2O. Since the energies of the triplet-state products are lower than those of the corresponding singlet-state products, the reaction is more liable to yield triplet-state products. Therefore, although most of the singlet-state intermediates and transition states are predicted to be at lower energy levels than the corresponding triplet-state structures, the feasible reaction may proceed along the triplet-state PES.

4. Conclusion

The detailed triplet potential energy surface of the reaction of $Ni(^3D) + H_2 + CO_2 \rightarrow Ni(^3D) + H_2O + CO$ is carried out at the CCSD(T)//B3LYP/6-311+G(2d,2p) levels. The main conclusions can be summarized as follows:

1. H_2 molecule and CO_2 can co-attach to one Ni atom with the formation of two different stable H_2NiCO_2 co-complexes (a-H_2NiCO_2 and b- H_2NiCO_2) in the predicted reaction coordinate, and only via the a-H_2NiCO_2 co-complex can the Ni insertion into the C−O bond of CO_2 proceed.

2. It is predicted that the dissociation of coordinated CO_2 molecule is prior to the dissociation of co-attached H_2 molecule. The H_2 moiety may promote the charge transfer in the Ni insertion process and facilitate the cleavage of C−O bond of CO_2 by reducing the energy barrier height.

3. The overall RWGS reaction over Ni catalyst is predicted to be endothermic by 12.5 kJ mol^{-1} with an energy barrier of 103.9 kJ mol^{-1}. The rate-determining step (RDS) for the entire reaction is predicted to be the hydrogen migration with water formation, which is remarkably different from that of the Ni insertion step for the $H_2/CO_2/Ni(^1S)$ system.

Acknowledgment. This work is financially supported by the Teaching and Research Award Program for Outstanding Young Teachers in Higher Education Institutions of MOE, People's Republic of China (2002), the Key Project of National Fundamental Research and Development of China (973) (No. G1999022407), NNSF (No. 20243006), and the Special Research Foundation of Doctoral Education of China (No. 2000061028).

Supporting Information Available: Vibrational frequencies of various compounds in the $Ni(^3D) + H_2 + CO_2$ reaction calculated at the B3LYP/6-311+G(2d, 2p) level and standard orientation for all optimized structures. This material is available free of charge via the Internet at http://pubs.acs.org.

References and Notes

(1) Weatherbee, G. D.; Barthlomew, C. H. *J. Catal.* **1981**, *68*, 67.
(2) Vance, C. K.; Barthlomew, C. H. *Appl. Catal.* **1983**, *7*, 169.
(3) Weatherbee, G. D.; Barthlomew, C. H. *J. Catal.* **1984**, *87*, 352.
(4) Luengo, C. A.; Cabrere, A. L.; Mackay, H. B.; Maple, M. B. *J. Catal.* **1977**, *47* 1.
(5) Schild, C.; Wokaun, A.; Koeppel, R. A. Biker, A. *J. Phys. Chem.* **1991**, *95*, 6341.
(6) Weatherbee, G. D.; Barthlomew, C. H. *J. Catal.* **1982**, *77*, 460.
(7) Fujita, S.-I.; Nakamura, M.; Doi, T.; Takezawa, N. *Appl. Catal. A: Gen.* **1993**, *104*, 87.
(8) Martin, G. A.; Primet, M.; Dalmon, J. A. *J. Catal.* **1978**, *53*, 321.
(9) Peebles, D. E.; Googman, D. F.; White, J. M. *J. Phys. Chem.* **1983**, *87*, 4378.
(10) Fujita, S.-I.; Terunuma, H.; Nakamura, M.; Takezawa, N. *Ind. Eng. Chem. Res.* **1991**, *30*, 1146.
(11) Campbell, T. K.; Falconer, J. L. *Appl. Catal.* **1989**, *50*, 189.
(12) Osaki, T.; Narita, N.; Horiuchi, T.; Sugiyama, T.; Masuda, H. Suzuki, K. *J. Mol. Catal. A: Chem.* **1997**, *125*, 63.
(13) Mascetti, J.; Tranquille, M. *J. Phys. Chem.* **1988**, *92*, 2177.
(14) Zhou, M.; Liang, B.; Andrews, L. *J. Phys. Chem. A* **1999**, *103*, 2013.
(15) Solymosi, F. *J. Mol. Catal.* **1991**, *65*, 337.
(16) Freund, H. J.; Messmer, R. P. *Surf. Sci.* **1986**, *172*, 1.
(17) Bartos, B.; Freund, H. J. *Surf. Sci.* **1987**, *179*, 59.
(18) Messmer, R. P.; Freund, H. J. In *Catalytic Activation of Carbon Dioxide*; Ayer, W. M., Ed.; American Chemical Society: Washington, DC, 1988; p 16.
(19) Hu, C.; Hu, H.; Li, M.; Tian, A. *J. Mol. Struct. (THEOCHEM)* **1999**, *491*, 155.
(20) Galan, F.; Fouassier, M.; Tranquille, M.; Mascetti, J.; Pápai, I. *J. Phys. Chem. A* **1997**, *101*, 2626.
(21) Mebel, A. M.; Hwang, D. Y. *J. Phys. Chem. A* **2000**, *104*, 11622.
(22) Hannachi, Y.; Mascetti, J.; Sitrling, A.; Pápai, I. *J. Phys. Chem. A* **2003**, *107*, 6708.
(23) Qin, S.; Hu, C.; Yang, H. *J. Theor. Comput. Chem.*, **2005**, *4*, 449−459.
(24) Armentrout, P. B. *Science* **1991**, *251*, 175.
(25) Eller, K.; Schwarz, H. *Chem. Rev.* **1991**, *91*, 1121.
(26) Roth, L. M.; Freiser, B. S. *Mass Spectrom. Rev.* **1991**, *10*, 303.
(27) Weisshaar, J. C. *Acc. Chem. Res.* **1993**, *26*, 313.
(28) Yoshihiti, S.; Kazunari, Y. *J. Am. Chem. Soc.* **2000**, *122*, 12317.
(29) Hwang, D. Y.; Mebel, A. M. *J. Phys. Chem. A* **2003**, *107*, 5092.
(30) Jenug, G.-H. *Chem. Phys. Lett.* **1995**, *232*, 319.
(31) Hwang, D. Y.; Mebel, A. M. *Chem. Phys. Lett.* **2000**, *325*, 639.
(32) Hwang, D. Y.; Mebel, A. M. *J. Phys. Chem. A* **2000**, *104*, 7646.
(33) Hwang, D. Y.; Mebel, A. M. *Chem. Phys. Lett.* **2002**, *357*, 50.
(34) Pápai, I.; Mascetti, J.; Fouriner, R. *J. Phys. Chem. A* **1997**, *101*, 4465.
(35) Sodupe, M.; Branchadell, V.; Oliva, A. *J. Mol. Struct. (THEOCHEM)* **1996**, *371*, 79.
(36) Pápai, I.; Schubert, G.; Hannachi, Y.; Mascetti, J. *J. Phys. Chem. A* **2002**, *106*, 9551.
(37) Becke, A. D. *J. Chem. Phys.* **1993**, *98*, 5648.
(38) Lee, C.; Yang, W.; Parr, R. G. *Phys. Rev. B* **1988**, *37*, 785.
(39) Stephens, P. J.; Devlin, F. J.; Chabalowski, C. F.; Frisch, M. J. *J. Phys. Chem.* **1994**, *98*, 11623.
(40) Pople, J. A.; Scott, A. P.; Wong, M. W.; Radom, L. *Isr. J. Chem.* **1993**, *33*, 345.
(41) Gonzalez, C.; Schlegel, H. B. *J. Chem. Phys.* **1989**, *90*, 2154.
(42) Purvis, G. D.; Bartlett, R. J. *J. Chem. Phys.* **1982**, *76*, 1910.
(43) Pople, J. A.; Head-Gordon, M.; Raghavachari, K. *J. Phys. Chem.* **1987**, *87*, 5968.
(44) Frisch, M. J.; Trucks, G. W.; Schlegel, H. B.; Scuseria, G. E.; Robb, M. A.; Cheeseman, J. R.; Montgomery, J. A., Jr.; Vreven, T.; Kudin, K. N.; Burant, J. C.; Millam, J. M.; Iyengar, S. S.; J. Tomasi, J.; Barone, V.; Mennucci, B.; Cossi, M.; Scalmani, G.; Rega, N.; Petersson, G. A.; Nakatsuji, H.; Hada, M.; Ehara, M.; Toyota, K.; Fukuda, R.; Hasegawa, J.; Ishida, M.; Nakajima, T.; Honda, Y.; Kitao, O.; Nakai, H.; Klene, M.; Li, X.; Knox, J. E.; Hratchian, H. P.; Cross, J. B.; Adamo, C.; Jaramillo, J.; Gomperts, R.; Stratmann, R. E.; Yazyev, O.; Austin, A. J.; Cammi, R.; Pomelli, C.; Ochterski, J. W.; Ayala, P. Y.; Morokuma, K.; Voth, G. A.; Salvador, P.; Dannenberg, J. J.; Zakrzewski, V. G.; Dapprich, S.; Daniels, A. D.; Strain, M. C.; Farkas, O.; Malick, D. K.; Rabuck, A. D.; Raghavachari, K.; Foresman, J. B.; Ortiz, J. V.; Cui, Q.; Baboul, A. G.; Clifford, S.; Cioslowski, J.; Stefanov, B. B.; Liu, G.; Liashenko, A.; Piskorz, P.; Komaromi, I.; Martin, R. L.; Fox, D. J.; Keith, T.; Al-Laham, M. A.; Peng, C. Y.; Nanayakkara, A.; Challacombe, M.; Gill, P. M. W.; Johnson, B.; Chen, W.; Wong, M. W.; Gonzalez, C.; Pople, J. A. *Gaussian 03*, revision B.05; Gaussian, Inc.: Pittsburgh, PA, 2003.
(45) Burghgraf, H.; Jansen, A. P. J.; Santen, R. A. V. *J. Chem. Phys.* **1994**, *101*, 11012.